pp 1592–1614.
doi:10.1017/aer.2020.57

Loss determination at a linear cascade under consideration of thermal effects

S. Aberle-Kern and R. Niehuis
svenja.aberle@unibw.de
Institute of Jet Propulsion
Universität der Bundeswehr München
85577 Neubiberg
Germany

T. Ripplinger
GE Aviation, Thermal & Combustion Systems
85748 Garching
Germany

ABSTRACT

Targeting higher efficiencies and lower fuel consumption of turbomachines, heat transfer and profile loss are research topics of particular interest. In contrast to that, the interaction of both was, so far, rarely investigated, but gains in importance in recent research activities. The profile loss of engine components can be characterised by the airfoil wakes at the blade rows utilising established measurement and evaluation methods for which an adiabatic flow is typically supposed. To enable the investigation of the influence of heat transfer at the blade on the loss characteristics, a novel evaluation procedure was set up. In addition to the pneumatic data, the total temperature in the airfoil wake at a linear cascade was measured by means of a five-hole probe with an integrated thermocouple. For the evaluation and analysis of these data, different definitions of the loss coefficient were investigated and, finally, extended to account for thermal aspects. Furthermore, established techniques to average the local wake data were applied and compared with special focus to their suitability for non-adiabatic cases. Moreover, an extended version of the mixed-out average as defined by Amecke was utilised applying not only a far-reaching consideration of a temperature gradient but also the inclusion of the third spatial dimension to enable the evaluation of field traverses in addition to single wake traverses. These techniques were applied to wake measurement data from a linear compressor cascade gained in a special test set-up in the high-speed cascade wind tunnel for different operating points and different blade temperatures. The suitability of the new methods could be proven, and initial steps of the aerodynamic analysis of the resulting data are presented. Thereby, the acquired techniques turned out as powerful methods for the evaluation of wake traverses on compressor and turbine cascades under non-adiabatic conditions.

Keywords: Mixed-out averaging; energy loss coefficient; linear cascade; thermal wake

Received 20 November 2019; revised 29 May 2020; accepted 5 June 2020.
A version of this paper was presented at the 24th ISABE Conference in Canberra, Australia, September 2019.

NOMENCLATURE

avg.	average
ISA	Institute of Jet Propulsion
HGK	high-speed cascade wind tunnel
CFD	computational fluid dynamics

Symbols

A	area
c	flow velocity
c_p	specific heat capacity
E	Energy
F	force
f	function
h	specific enthalphy
I	integral
i	numeric counter
$\dot{m}$	mass flow rate
N	number of measurement points
p	pressure
P	momentum
q	aerodynamic: stagnation pressure
q	thermodynamic: heating power
R	specific gas constant
ρ	density
s	specific entropy
t	pitch
T	Temperature
ϵ	error
ζ	loss coefficient
κ	heat capacity ratio
Δ	difference
Ω	any flow quantity

Subscripts/Superscripts

a	area-weighted average
A	Amecke average
C	compressor
f	function
h	energy/enthalpy
hq	extended enthalpy
I	integral

https://doi.org/10.1017/aer.2020.57 Published online by Cambridge University Press

i	numeric counter
$loss$	loss
m	mass flow-weighted average
mo	complete mixed-out average
p	total pressure
q	non-adiabatic/after heat application
s	thermodynamic: isentropic
s	loss coefficient: entropy
t	total
T	Turbine
u	pitch-wise direction
x	axial direction
z	span-wise direction
Ω	any flow quantity
1	Section 1 (inflow)
2	Section 2 (outflow)
1,2,3,4,5	numeric index
–	averged
∞	mixed-out state at infinity

1.0 INTRODUCTION

Lower fuel consumption and reduced emissions are a major target of nowadays aeronautical engineering. As the efficiency of a jet engine is highly depending on the temperature management in specific engine components, the research on heat transfer phenomena and cooling efficiencies gains in importance. The Institute of Jet Propulsion at the Bundeswehr University Munich has been conducting research into heat transfer at linear cascades for many years, e.g. by Gomes and Niehuis[1]. Furthermore, the investigation of the wake and loss mechanisms is part of basic studies for each cascade. So far, only pneumatic data of the wake were acquired while a possible variation of the temperature in the wake was neglected for the determination of the loss coefficient. This raises the question as to what extent this assumption is justified, particularly in cases with considerable temperature differences between the investigated blade and the flow which may increasingly occur with new engine concepts.

Details on established definitions of the loss coefficient are revealed by Denton[2]. Beside the discussion of different physical mechanisms of loss, he mainly distinguishes between three different possibilities of its quantification: The energy loss coefficient, the entropy loss coefficient and the total pressure loss coefficient. The latter one is the most common type of loss definition in turbomachinery and is typically used at the ISA, as for instance by Stotz et al.,[3] and at other institutes, as e.g. by Schobeiri et al.[4] However, other researchers prefer to utilise the entropy loss coefficient, such as at the Whittle Laboratory at the University of Cambridge, for example in the publications by Lim et al.[5] or Gunn and Hall[6]. Of course, the usage of all of these approaches can be justified, but their meanings vary in the details which should be considered while using the one or the other, as is revealed in this paper.

https://doi.org/10.1017/aer.2020.57 Published online by Cambridge University Press

The loss can be quantified as local or global values. It is typically derived from the airfoil wake where the local loss can be determined for discrete positions and the global loss is calculated as an averaged value for the respective wake, which allows for a facilitated assessment of the determined loss coefficient in comparing different test cases. In order to calculate the averaged value, different approaches are commonly used for different purposes, discussed by Cumpsty and Horlock[7]. Beside the frequently used area-weighted average and mass-flow weighted average, the mixed-out average according to Amecke[8] is particularly popular for cascade testing. Following this work, an advanced approach for the mixed-out average in three-dimensional engine components was presented by Prasad et al.[9]

As the mentioned techniques to quantify the loss in a turbomachine blade row are typically based on the assumption of an adiabatic case, their suitability for non-adiabatic conditions has to be reassessed in detail. For investigations with film cooling, Gomes and Niehuis[1] have shown an approach to correct the total pressure loss coefficient by the added cooling air mass flow. Furthermore, Lim et al.[5] revealed a method, to determine the entropy loss coefficient in cases with film cooling, by considering a separate entropy increase due to the thermal and aerodynamic mixing of the added coolant air utilising its mass flow rate and temperature. This approach, however, is not suitable for non-adiabatic cases without added air mass flow, as the presented additional entropy terms would be zero. Additionally, this approach requires the knowledge of an uncooled reference case.

In this paper, experimental data from a linear cascade of compressor vanes are used for a discussion of different definitions of the loss coefficient under non-adiabatic condition. Further investigations on the profile loss at linear cascades of compressor vane airfoils under adiabatic conditions were conducted by Leipold et al.[10] and Hilgenfeld et al.[11] As an evaluation criterium the Amecke averaged total pressure loss coefficient[8], calculated from data of wake traverses, is frequently used in their work. These experimental studies were utilised as a test case for numerical investigations by Leggett et al.[12] in order to quantify the quality of loss prediction by means of advanced numerical simulations. In their analyses, the total pressure loss coefficient is used as well, whereas a method of calculation based on the displacement thickness and on the momentum thickness of the airfoil boundary layer is utilised which was already suggested by Denton[2]. Beside advantages of this technique due to boundary conditions in the numerical simulation, this approach facilitates the additional investigation of the impact of loss sources. As an averaging technique, they use either the mixed-out average for clean inlet cases or the mass flow-weighted average in cases with inlet distortion. The loss determination by means of boundary layer data according to Denton[2] was also performed in an experimental set-up on a linear low-pressure turbine cascade by Howell and Roman[13], as a total pressure measurement in the wake could not be performed due to geometric constraints.

Turning the focus back to the more common method of loss determination by means of wake traverses and, in particular, on the influence of a heat transfer at the blade on the loss, a temperature measurement in the wake is required. Provided that pneumatic and thermal data are available, the established evaluation criteria for the loss characteristics have to be reconsidered concerning validity and suitability. This does not only concern the definition of the loss coefficient but also the averaging techniques. After discussing the established methods of both, possibilities for their extension to non-adiabatic cases are deduced and discussed. The main objective of this paper is to set up and present reliable methods for the profile loss determination at non-adiabatic blade rows which meet the following constraints:

https://doi.org/10.1017/aer.2020.57 Published online by Cambridge University Press

1. Thermodynamic validity
2. Independency from adiabatic reference cases
3. Determinability by means of wake traverses without inlet distortion

The suitability of these novel methods is then evaluated for exemplary wake measurements on a linear compressor cascade with a heated center blade. However, it is expected that the findings are not limited to the application on compressor blade rows but can also be utilised for turbine cascades. The calculation procedure for both cases is presented.

2.0 DETERMINATION OF LOSS

In turbomachinery components, there are several different mechanisms interacting which cause losses. Before revealing different types of loss determination, its origin is discussed first.

With respect to thermodynamics, the lossy Joule-Brayton cycle is characterised by an increase of entropy during compression as well as during expansion. Losses in the combustion system, such as the loss of total pressure and burn-off loss, are not further discussed in this paper. In Fig. 1, the basic thermodynamic change of state of compression and expansion are shown for a stationary blade row under adiabatic conditions.

The isentropic change of state 1→2s is often referred to as lossless, whereas the real, polytropic change 1→2 underlies the generation of entropy resulting in a higher effort of enthalpy concerning the compressor or a lower usable enthalpy concerning the turbine. The difference of both states 2s and 2 is usually referred to as the loss h_{loss}. For a relative comparison of differently shaped engine components, the loss is typically related to the effort of kinetic flow energy at the inlet concerning a compressor or the total usable kinetic energy at the outlet concerning a turbine, as revealed in Equation 1. This differentiation is intuitive regarding the entire engine while the known boundary conditions are at the inlet for the compressor and at the outlet for the turbine.

$$\text{Compressor: } \zeta_C = \frac{h_{loss}}{c_1^2/2} \quad \ldots (1a)$$

$$\text{Turbine: } \zeta_T = \frac{h_{loss}}{c_2^2/2} \quad \ldots (1b)$$

2.1 Quantification of loss

To quantify the profile loss at a turbomachine component, different definitions of loss coefficients have been established for different applications. Denton[2] emphasises three commonly used definitions based on:

1. energy
2. entropy
3. total pressure

For adiabatic cases, the energy loss coefficient is a measure of the utilisation of the kinetic energy. Setting up the first law of thermodynamics in Equation 2 based on Fig. 1, the understanding of the definition of the energy loss coefficient in Equation 3a and 3b according

https://doi.org/10.1017/aer.2020.57 Published online by Cambridge University Press

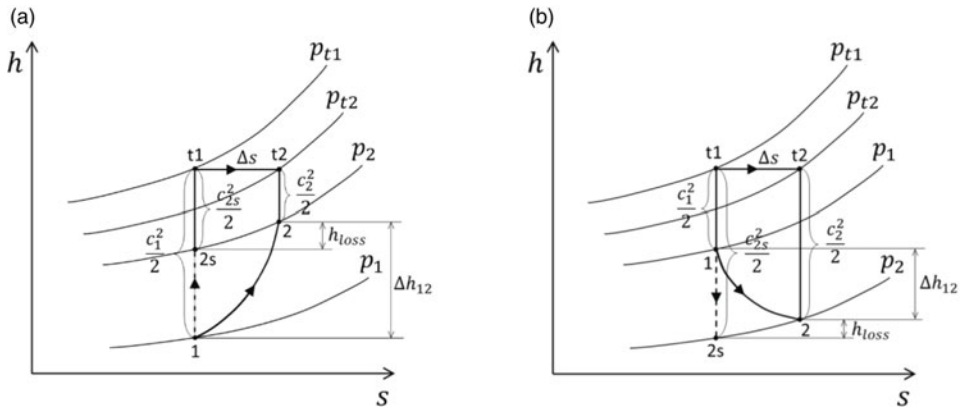

Figure 1. Exemplary enthalpy–entropy diagram for an adiabatic compression and expansion at a stationary blade row. (a) Compressor. (b) Turbine.

to Denton[2] is facilitated. The loss of kinetic energy and of enthalpy can be regarded synonymously at an adiabatic flow.

$$\frac{c_1^2}{2} = \Delta h_{12} + \frac{c_2^2}{2} = \Delta h_{12} + \frac{c_{2s}^2}{2} - h_{loss} \quad \ldots (2)$$

$$\text{Compressor: } \zeta_{h,C} = \frac{c_{2s}^2/2 - c_2^2/2}{c_1^2/2} = \frac{h_2 - h_{2s}}{h_{t1} - h_1} = \frac{h_{loss}}{h_{t1} - h_1} \quad \ldots (3a)$$

$$\text{Turbine: } \zeta_{h,T} = \frac{c_{2s}^2/2 - c_2^2/2}{c_2^2/2} = \frac{h_2 - h_{2s}}{h_{t2} - h_2} = \frac{h_{loss}}{h_{t2} - h_2} \quad \ldots (3b)$$

A second way of loss quantification is the entropy loss coefficient by which the loss is directly related to the generation of entropy as in Equation 4. Assuming air as an ideal gas, the entropy generation can be calculated by Equation 5.

$$h_{loss} = \int_{s_1}^{s_2} T ds \approx T_2 \cdot \Delta s_{12} \quad \ldots (4)$$

$$\Delta s_{12} = c_p \cdot \ln \frac{T_{t2}}{T_{t1}} - R \cdot \ln \frac{p_{t2}}{p_{t1}}. \quad \ldots (5)$$

The resulting entropy loss coefficient is defined in Equations 6a and 6b[2].

$$\text{Compressor: } \zeta_{s,C} = \frac{T_2 \cdot \Delta s_{12}}{h_{t1} - h_1} \quad \ldots (6a)$$

$$\text{Turbine: } \zeta_{s,T} = \frac{T_2 \cdot \Delta s_{12}}{h_{t2} - h_2} \quad \ldots (6b)$$

https://doi.org/10.1017/aer.2020.57 Published online by Cambridge University Press

Finally, the most common definition of the loss coefficient is given by the total pressure loss coefficient in Equations 7a and 7b[2]. It results from the energy loss coefficient, assuming an incompressible flow.

$$\text{Compressor: } \zeta_{p,C} = \frac{\rho c_{2s}^2/2 - \rho c_2^2/2}{\rho c_1^2/2} = \frac{q_{2s} - q_2}{q_1} = \frac{p_{t1} - p_{t2}}{p_{t1} - p_1} \quad \ldots (7a)$$

$$\text{Turbine: } \zeta_{p,T} = \frac{\rho c_{2s}^2/2 - \rho c_2^2/2}{\rho c_2^2/2} = \frac{q_{2s} - q_2}{q_2} = \frac{p_{t1} - p_{t2}}{p_{t2} - p_2} \quad \ldots (7b)$$

To determine the mentioned loss coefficients for a test object, primarily the values of total and static pressure have to be determined upstream and downstream of the test object. Assuming $T_{t2} = T_{t1}$ for adiabatic cases, the temperature information in the wake, which is necessary for the energy and entropy loss coefficient, can be calculated from the pressure data and the inlet total temperature. Thus, the measurement of the total temperature in the wake is not obligatory in experimental setups, although it could deliver helpful additional information, as shown later on.

Denton[2] has shown that the energy and entropy loss coefficients have to be approximately equal. The justification of the entropy loss coefficient is according to Denton[2] that the summation of the created entropy in each blade row is valid to be assumed as the entropy created in the whole machine, whereas values of total pressure or total enthalpy depend on its relative frame, either rotating or stationary. Moreover, all three mentioned definitions of the loss coefficient deliver the same result for incompressible flows under adiabatic conditions.

2.2 Averaging methods

For the calculation and comparison of the former mentioned loss coefficients, the values of total and static pressure as well as total and static temperature, if desired or necessary, have to be determined for the inflow Section 1 and the outflow Section 2. Regarding the investigation of a two-dimensional blade row, the inflow pressure at Section 1 is typically homogeneous, whereas the outflow field at Sections 2a and 2b is characterised by the wake, as illustrated in Fig. 2. In this paper, cases without inlet distortion are discussed, but the averaging techniques presented below can be applied similarly for non-uniform inlet flow parameter.

To quantify the loss, the local loss coefficient can be determined according to the discrete distribution of pressure and temperature along the pitch. This may give information about height and width of the wake peak. However, in order to compare the loss of different cascades or different operating points appropriately, there are several established averaging techniques for the characterising parameters of the wake typically used[14].

According to Cumpsty and Horlock[7], the appropriate averaging method depends on the context of evaluation and the intended purpose. The first discussed example is the area-weighted average, which is only valid for static pressure information, interpreting $F = \overline{p} \cdot A$ as the net force on the outlet area A[7]. Nevertheless, it is commonly used for the total pressure or the total temperature as well for practical reasons, as its determination is straightforward. This can be justified in several cases, for example if separation regions are negligible[7].

https://doi.org/10.1017/aer.2020.57 Published online by Cambridge University Press

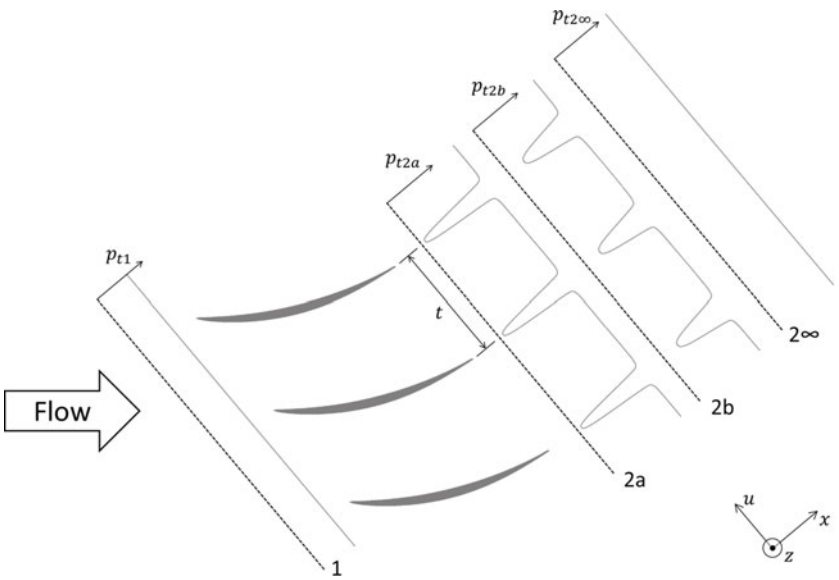

Figure 2. Illustration of wake measurement planes at a linear cascade (airfoil not to scale)

Accordingly, the area-weighted loss coefficient is determined by the averaged flow quantities $\Omega \in \{p_2\ , p_{t2}, T_2, T_{t2}\}$ as shown in Equation 8

$$\overline{\Omega}^a = \frac{1}{t} \int_0^t \Omega du. \qquad \ldots (8)$$

A second common method is the mass flow-weighted average. The previously discussed loss definitions are based on enthalpy considerations, which are defined per unit mass.[7] By the mass flow-weighted average, the consideration of a mass deficit in a boundary layer as a reduced enthalpy flux instead of a direct loss is possible. Hence, it is valid for total temperature information and can be transferred to total pressure distributions, if its variations in the wake are comparably low[7]. The resulting mass flow-weighted loss coefficient is defined by the averaged flow quantities Ω in Equation 9

$$\overline{\Omega}^m = \frac{\frac{1}{t}\int_0^t \Omega \cdot \rho_2 c_{x,2} du}{\frac{1}{t}\int_0^t \rho_2 c_{x,2} du}. \qquad \ldots (9)$$

Particularly for two-dimensional cascade testing, Cumpsty and Horlock[7] emphasise another averaging method, which is the mixed-out average according to Amecke[8]. The hypothetical mixed-out state at infinity in Section 2∞ of static and total pressure as well as the two-dimensional flow direction is calculated by Amecke[8] analytically under consideration of mass conservation in Equation 10 and momentum conservation in axial flow direction x in Equation 11 as well as in pitch-wise direction u in Equation 12, each set up between Sections 2a or 2b respectively and Section 2∞ (cf. Fig. 2).

https://doi.org/10.1017/aer.2020.57 Published online by Cambridge University Press

$$\dot{m}_{2\infty} = \dot{m}_2 \quad \Leftrightarrow \quad \rho_{2\infty} \cdot c_{x,2\infty} = \frac{1}{t}\int_0^t \rho_2 \cdot c_{x,2} du \qquad \ldots(10)$$

$$P_{x,2\infty} = P_{x,2} \quad \Leftrightarrow \quad \rho_{2\infty} \cdot c_{x,2\infty}^2 + p_{2\infty} = \frac{1}{t}\int_0^t \rho_2 \cdot c_{x,2}^2 + p_2 du \qquad \ldots(11)$$

$$P_{u,2\infty} = P_{u,2} \quad \Leftrightarrow \quad \rho_{2\infty} \cdot c_{x,2\infty} \cdot c_{u,2\infty} = \frac{1}{t}\int_0^t \rho_2 \cdot c_{x,2} \cdot c_{u,2} du. \qquad \ldots(12)$$

Using this approach, averaged values can be understood as synonymous with the data in the mixed-out state. The shown integrals can be determined straightforward from the wake in experimental or numerical investigations while utilising the trapezoidal rule for spatially discretised data. The solution of the three equations depending on the known integrated wake data leads to the three unknown parameters in the assumed mixed-out state $c_{x,2\infty}$, $c_{u,2\infty}$ and $p_{2\infty}$, applying $T_{t,2\infty} = T_{t1}$. Amecke[8] noted the corresponding energy conservation additionally, but assumed a negligible temperature variation in the wake and showed that this makes the energy conservation obsolete. By means of the results of these equations, the loss coefficients $\bar{\zeta}^A$ can be determined according to the above-mentioned definitions[8].

One of the major advantages of the Amecke averaging is that the determined flow values in the mixed-out state and, therefore, the determined averaged loss coefficients are theoretically independent of the axial location of measurement downstream of the cascade. This means that the wake traverse at Section 2a delivers the same mixed-out loss coefficient as the measurement in Section 2b, as no change in mass, momentum or energy occurs between the two areas. However, a drawback of the Amecke approach is that it is not valid anymore, if temperature gradients inside the wake are high, i.e. in cases of heated or cooled blades. Additionally, the existing approach is two-dimensional and, thus, not valid for field traverses with three-dimensional flow phenomena.

2.3 Overcoming the limits for non-adiabatic cases

Many experimental and numerical investigations of turbomachine components meet the assumption of an adiabatic structure. Triggered by the intended investigation of the interaction of heat transfer and aerodynamic loss, the established evaluation methods had to be revisited. Deriving methods for the loss determination at non-adiabatic test cases is an essential step to enable the thermodynamic assessment of thereby occurring loss mechanisms.

2.3.1 Effects to the loss coefficient

Dealing with non-adiabatic cases in a turbomachinery component may have different reasons that have to be evaluated specifically. In the case of a compressor, a heat flux through the casing is often not avoidable but might be of negligible order at least for low-pressure compressors. Regarding a turbine, blades and casing are often actively cooled. The heat flux is comparably high and achieved by an additional effort. Evaluating the loss coefficient by the above-mentioned equations, the cooling effort would be counted as subtracted loss, which

https://doi.org/10.1017/aer.2020.57 Published online by Cambridge University Press

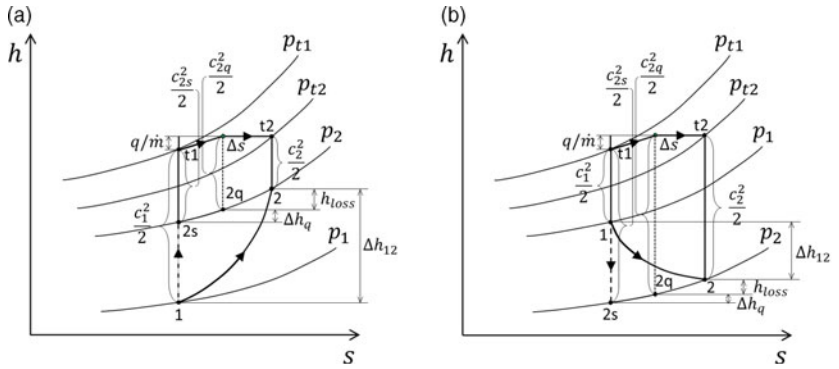

Figure 3. Enthalpy–entropy diagram for a non-adiabatic compression and expansion. (a) Compressor. (b) Turbine.

may impede its correct interpretation. The same argument applies accordingly for the active heating of engine components. For this special case, the thermodynamics of a non-adiabatic compression or expansion with heat addition is revealed in Fig. 3. The effects of a cooling are analogous.

It should be considered that the heat application and the aerodynamic loss generation are commutative in thermodynamic regard. From this point of view, it is not relevant, if the addition of heat is considered before the aerodynamic loss, or the other way around, or if both processes are considered in parallel. Based on this assumption, the modified changes of state are evaluated as follows.

The amount of heat flux can be calculated as the local increase of total enthalpy in the wake according to Equation 13 while a constant specific heat capacity c_p is assumed for low temperature variations. Considering a homogeneous heat flux over the entire blade, this is equal to the total induced heating power per air mass flow over the entire blade.

$$\frac{q}{\dot{m}} = \Delta h_t = c_p \cdot \left(\overline{T_{t2}} - T_{t1}\right). \qquad \ldots (13)$$

As a consequence of the heat transfer, the energy conservation is modified according to Fig. 3 in Equation 14.

$$\frac{c_1^2}{2} + \frac{q}{\dot{m}} = \Delta h_{12} + \frac{c_2^2}{2} = \Delta h_{12} + \frac{c_{2s}^2}{2} - h_{loss} + \underbrace{\frac{q}{\dot{m}} - \Delta h_q}_{\frac{\Delta c_{2q}^2}{2}}. \qquad \ldots (14)$$

The above-introduced energy loss coefficient for the adiabatic case can be interpreted as a measure of the utilisation of the kinetic energy, as shown in Equation 3. For the non-adiabatic case, it is obvious that the heat application implies a flow acceleration by Δc_{2q}. Hence, the loss of enthalpy is not equal to the loss of kinetic energy for non-adiabatic cases. This is a very important fact, to keep in mind for the consideration of a suitable measure of loss.

Heading back to the explanation of Denton[2], a deviation from isentropic flow inevitably involves a reduction of efficiency. In that respect, the addition of heat unavoidably leads to an increase of entropy according to the Rayleigh line[15]. Thus, the heating of a flow is never lossless, even under otherwise ideal conditions. Therefore, the evaluation of the transformation

https://doi.org/10.1017/aer.2020.57 Published online by Cambridge University Press

of heat into kinetic energy is not fully reasonable, as it physically can never occur completely. More meaningful for investigations in turbomachinery is the state of static enthalpy. Hence, the extended enthalpy loss coefficient is defined in Equation 15 with respect to Fig. 3.

$$\text{Compressor: } \zeta_{hq,C} = \frac{h_2 - h_{2s} - \Delta h_q}{h_{t1} - h_1} \quad \ldots (15a)$$

$$\text{Turbine: } \zeta_{hq,T} = \frac{h_2 - h_{2s} - \Delta h_q}{h_{t2} - h_2} \quad \ldots (15b)$$

For typical investigations, the total and static quantities at inlet Section 1 and outlet Section 2 are known. The more complex process in between includes a loss of total pressure due to the polytropic change of state as well as by the application of heat. In parallel, both processes underlie a creation of entropy. As indicated above, it does not matter which part of the loss is caused by one of the two overlapping effects in order to find a suitable calculation method for an enthalpy loss coefficient. Eventually, the real outlet conditions in Section 2 are related to the process under ideal conditions which is isentropic compression or expansion to state 2s and isobaric application of heat to state 2q, as illustrated in Fig. 3. From these considerations the increase of static enthalpy due to the application of heat can be calculated by Equation 16.

$$\Delta h_q = h_{2q} - h_{2s} = c_p \cdot \left(T_{2q} - T_{2s}\right) \quad \ldots (16)$$

The static temperature and flow velocity for the theoretical isentropic case are determined by Equations 17 and 18 with $T_{2s} = T_1 \cdot (p_2/p_1)^{\frac{\kappa-1}{\kappa}}$.

$$T_{2s} = T_{t1} - \frac{c_{2s}^2}{2c_p} \quad \ldots (17)$$

$$\Rightarrow c_{2s} = \sqrt{2c_p \cdot (T_{t1} - T_{2s})} \quad \ldots (18)$$

The mass flow conservation in Equation 19 leads to the theoretical flow velocity after heat addition in Equation 20, provided that the theoretic areas are $A_{2q} = A_{2s}$ and that $p_{2q} = p_{2s}$ due to the isobaric addition of heat.

$$\rho_{2s} \cdot c_{2s} = \rho_{2q} \cdot c_{2q} \quad \ldots (19)$$

$$\Rightarrow c_{2q} = \frac{T_{2q}}{T_{2s}} \cdot c_{2s} \quad \ldots (20)$$

Finally, the theoretical static temperature after heat addition can be determined by Equation 21 and resolved by the quadratic formula in Equatoin 22.

$$T_{2q} = T_{t2} - \frac{c_{2q}^2}{2c_p} = T_{t2} - \left(\frac{T_{2q}}{T_{2s}}\right)^2 \cdot \frac{c_{2s}^2}{2c_p} \quad \ldots (21)$$

$$\Rightarrow T_{2q} = -\frac{c_p T_{2s}^2}{c_{2s}^2} \pm \sqrt{2c_{2s}^2 \cdot c_p T_{t2} + c_p^2 T_{2s}^2} \cdot \frac{T_{2s}}{c_{2s}^2} \quad \ldots (22)$$

https://doi.org/10.1017/aer.2020.57 Published online by Cambridge University Press

As it is obvious that a negative temperature is not reasonable, the positive solution in Equation 22 must be chosen. Hence, T_{2q} and T_{2s} can be applied in Equation 16 to determine Δh_q and, finally, ζ_{hq} from Equation 15. Furthermore, Equation 14 to 22 are valid analogously for the active cooling of a blade with a negative heat transfer $\Delta h_q < 0$. The entropy loss coefficient can be adapted similarly, leading to approximately equal results as was already shown for the adiabatic definition.

By means of this new definition, which is referred to as the *extended enthalpy loss coefficient* below, it is targeted to evaluate the aerodynamic performance of an engine component under non-adiabatic conditions independently from detailed thermal aspects.

2.3.2 Effects to averaging techniques

As the area-weighted average is only affected by the distribution of the variables for the loss coefficient themselves, the average calculation is independent from the adiabatic or non-adiabatic point of view. The mass flow-weighted average is indirectly influenced by a heat transfer as the mass flow density can vary as a consequence, which does not require a modified definition as well. Concerning the total pressure loss coefficient, it can be discussed, if it is reasonable to use the density distribution ρ_2 at the outflow or rather the density ρ_1 at the inlet for the calculation of the mass flow-weighted average, as the justification for the total pressure loss coefficient is the assumption of an incompressible flow. The authors decided to use $\rho = \rho_2$ for adiabatic and non-adiabatic cases for three reasons:

1. The inlet density ρ_1 can only vary due to, in the presented investigations, undesirable local or temporal variations in the experimental set-up and is otherwise constant. The intended correction of local mass flow variations in the wake is not fully possible assuming an incompressible flow, as only velocity variations are taken into account.
2. The total pressure loss coefficient is nowadays an established value for the evaluation of the aerodynamic performance, for incompressible flows as well as for obviously compressible flows. This is not wrong in the first instance, as long as the interpretation is based on the introduced stagnation pressure rather than on energetic arguments. Nevertheless, the density at outflow can vary considerably from the density at inflow. Thus, the mass flow-weighting for the average at outflow should be based on the correct density distribution in the wake.
3. A heat transfer over the blade row or entire component can have a distinctive impact on the density at outflow. This would be ignored if the weighting was performed by means of the inflow density, independent from the issue, whether the flow is compressible or incompressible.

Finally, the averaging approach of Amecke[8] is based on the neglected temperature variation in the wake, as mentioned above. To keep the basic idea valid, the method has to be extended. Apart from temperature gradients in the wake, also the third, span-wise dimension of the flow cannot be evaluated by the method of Amecke, which could be useful, particularly for wake traverses in regions of secondary flow. Besides, the utilisation of the third dimension of the flow can also improve the accuracy of single wake traverses at mid-span, as small yaw angles of the inflow cannot always be avoided. Thus, the equation for the third dimension of the momentum conservation is noted in Equation 23 as well as the energy conservation in Equation 24 which was already utilised by Kost.[16]

https://doi.org/10.1017/aer.2020.57 Published online by Cambridge University Press

$$P_{z,2\infty} = P_{z,2} \quad \Leftrightarrow \quad \rho_{2\infty} \cdot c_{x,2\infty} \cdot c_{z,2\infty} = \frac{1}{t} \int_0^t \rho_2 \cdot c_{x,2} \cdot c_{z,2} du \quad \ldots (23)$$

$$E_{2\infty} = E_2 \quad \Leftrightarrow \quad \rho_{2\infty} \cdot c_{x,2\infty} \cdot c_p \cdot T_{t2\infty} = \frac{1}{t} \int_0^t \rho_2 \cdot c_{x,2} \cdot c_p \cdot T_{t2} du \quad \ldots (24)$$

Taking the integrated values as known from the wake traverse utilising the trapezoidal rule, the five equations in Equations 10, 11, 12, 23 and 24 can be solved to the five unknown, averaged parameters $c_{x,2\infty}$, $c_{u,2\infty}$, $c_{z,2\infty}$, $p_{2\infty}$ and $T_{t2\infty}$ assumed in the theoretic mixed-out state. The resulting averaged loss coefficient $\overline{\zeta}^{mo}$ is referred to as the *complete mixed-out average* below. The presented demonstration is the first application of this extended averaging approach directly compared to the approach of Amecke[8] for adiabatic and non-adiabatic cases.

3.0 TEST SET-UP

For the investigation and assessment of different definitions of the loss coefficient as well as different averaging techniques, a multitude of experimental wake traverses were conducted in the high-speed cascade wind tunnel, at which a special compressor cascade with an optionally heated blade was implemented.

3.1 Test facility

The high-speed cascade wind-tunnel of the Institute of Jet Propulsion is shown schematically in Fig. 4, giving basic information on this special test facility in addition. It is an open-loop test facility with an open test section located inside a pressure tank. This enables the variation of the density inside the test facility and thus, the adjustment of Reynolds number and Mach number independently from each other. Therefore, it is ideally suitable for the investigation of basic aerodynamics on linear compressor or turbine cascades.

The unique test facility was put into service in 1955 under coordination of Schlichting[17] at the Deutsche Forschungsanstalt für Luftfahrt in Braunschweig, Germany. The entire wind-tunnel was moved in 1985 to the Institute of Jet Propulsion of the Bundeswehr University Munich while only minor constructional changes were made[18]. Since a major revision of the HGK in 2017, it is driven by a 1.8MW high voltage asynchronous motor with a frequency converter, see Fig. 4. By means of a mechanical transmission, it drives a three-stage axial compressor providing a maximum pressure ratio of 2.74. A bypass system enables lower mass flow rates in the test section than allowed by the compressor map by preventing the compressor from stalling. Depending on the variable channel height, this system provides a Mach number range from $Ma = 0.1$ to $Ma = 1$. Behind a diffuser a flap-controlled water cooler allows for a temperature control between 298 and 333K. In order to realise a homogenous flow field, a honeycomb mesh is installed inside the settling chamber, before the flow is accelerated in the nozzle to the desired Mach number at the test section. Optionally, various turbulence generators can be mounted inside the nozzle to achieve a defined turbulence level. By a rotatable ring at the section of measurement, the inflow angle towards the cascade can be adjusted.

https://doi.org/10.1017/aer.2020.57 Published online by Cambridge University Press

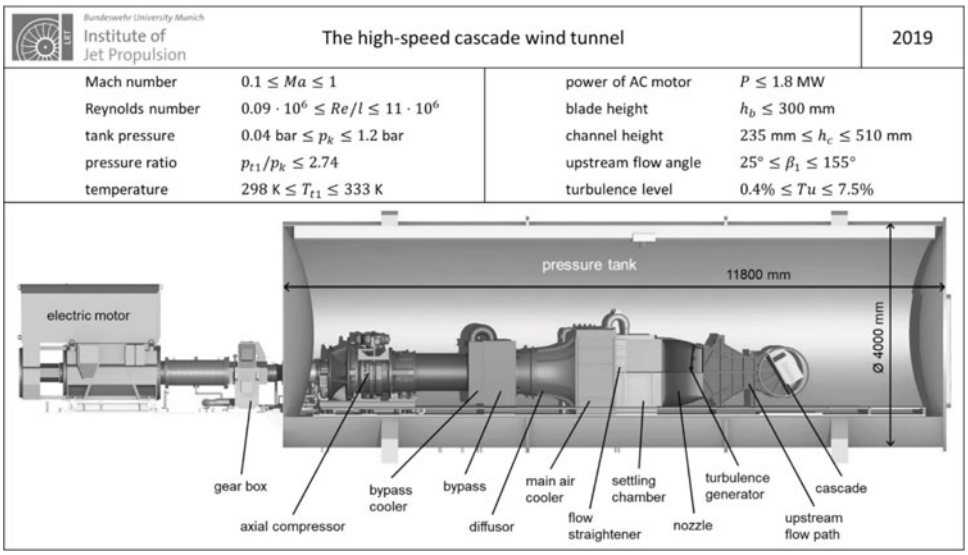

Figure 4. Schematic of the high-speed cascade wind tunnel at the ISA

For wake traverses by various types of probes, a four-axis traversing device is installed next to the test section. Beside the axis in flow direction and an axis perpendicular to that in blade span direction, the vertical axis can be aligned parallel to the cascade inlet plane. The fourth axis is a rotating axis in blade span direction enabling the alignment of the probe parallel to the main outflow direction.

3.2 Specific cascase set-up

The cascade under consideration here is based on a compressor vane, which is provided to the ISA by GE Aviation. For the presented test set-up, the center blade of the cascade is equipped with a heating system by means of an internal cycle of hot oil. Concerning the planned investigations, it is not primarily targeted to receive a homogeneous heat flux distribution on the blade, as necessary for measurements of the heat transfer coefficient. The heat transfer was measured at this cascade by a different set-up described by Aberle et al.[19]

In order to evaluate the performance of the cascade, wake traverses were conducted by means of an in-house designed five-hole probe with integrated thermocouple for a simultaneous measurement of pressure and temperature data. The thermocouple is placed within a Kiel-shroud on top of the five-hole probe head, as shown in Fig. 5. The probe was orientated parallel to the blades, such that temperature and pressure data are acquired synchronously at the same pitch-wise direction. By traversing the probe to in total 63 discrete positions along one pitch length downstream of the center blade, the wake can be characterised. The distance of adjacent measurement points is thereby between 0.25mm directly in the wake and 4mm in the distortion-free stream. At each measurement position, the pressure balancing of each pressure tap is monitored in order to ensure a reliable steady state measurement. Additionally, each measurement value is an average of several seconds of measurement to account for slight temporal variations of the flow parameter. A prerequisite is furthermore the continuous monitoring of the inflow parameters to provide a constant inflow.

https://doi.org/10.1017/aer.2020.57 Published online by Cambridge University Press

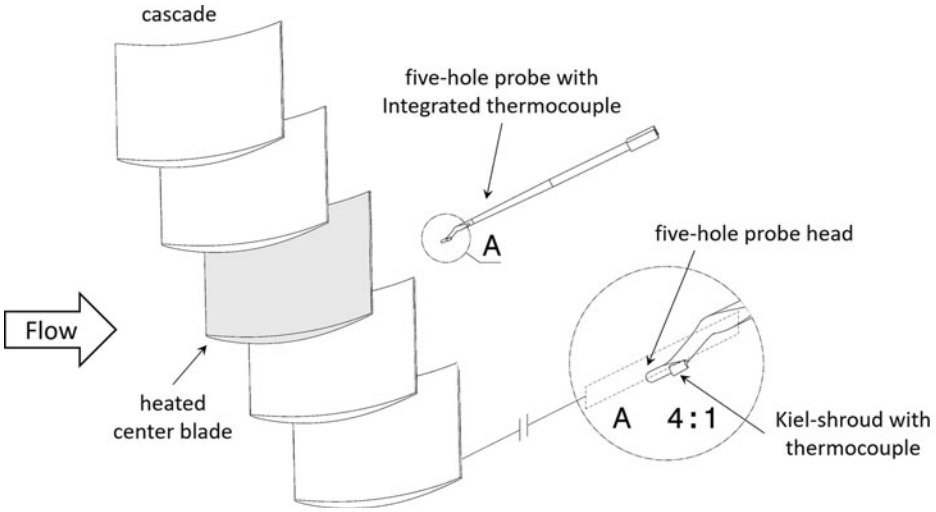

Figure 5. Illustration of cascade and probe alignment for wake traverses (airfoil not to scale)

The pressure data of the operating point at the HGK is acquired by multiple 98RK-1 rack-mount pressure scanners. A specific pressure module is chosen depending on the required pressure range to minimise measurement uncertainties. The inlet total temperature, however, is determined as a mean of four PT100 temperature sensors, one at each wall of the wind tunnel. With these four temperature values, the homogeneity of the inflow temperature can be furthermore monitored. For the presented tests, no turbulence generator is used. The remaining turbulence intensity is lower than 1%. As the investigation of inlet distortions is not targeted in the scope of the presented tests, a homogeneous inflow is ensured within the investigated range.

As to the five-hole probe data, the pressure values of the five-hole probe were measured by a PSI 9116 pressure scanner. Data from the type T class 1 thermocouple mounted on the probe was acquired by an NI ethernetRIO 9147 system utilizing an NI 9211 module. Both were mounted inside the tank of the HGK to keep tube and cable lengths low.

Beside the variation of inflow Reynolds and Mach number, the blade temperature was varied from cold state, which equals the inflow total temperature of 303.15K, to different degrees of hot state up to about 415K, as this is the order of magnitude of the application relevant temperature gradient. The corresponding heating power is determined by means of the temperature difference at the heating medium. Extensive insulations keep conductive losses low. The airfoil wakes were investigated for high-speed ($Ma_1 \gg 0,3$) as well as low-speed operating points ($Ma_1 < 0,3$). Additionally, several field traverses were conducted.

3.3 Measurement uncertainty

The estimation of measurement uncertainties gives an order of magnitude of the reliability of the results. Starting with the acquirement of raw data, the pressure values were determined by an accuracy of 3.8Pa for low inflow Mach numbers and by 17.2Pa for medium and high inflow Mach numbers according to the manufacturer's calibration of the pressure scanners. This accuracy applies for the inflow pressure measurement in the same way as for measurements in the outflow by means of the five-hole probe. The inlet total temperature is determined by an accuracy of 0.5K, including the entire measurement chain with sensors and acquisition

https://doi.org/10.1017/aer.2020.57 Published online by Cambridge University Press

device. The outflow temperature, determined by a thermocouple type T on the five-hole probe, is moreover influenced by the recovery factor which has to be calibrated properly. This was conducted inside the test facility providing an implicit calibration of the measurement chain including thermocouple and acquisition module. The remaining measurement uncertainty can be numbered to 0.5K.

Based on the measurement uncertainty of the raw data, a Gaussian error propagation according to Barlow[20] was conducted up to the evaluated five-hole probe results utilising: $\epsilon_f = \sqrt{\sum \left(\frac{\partial f}{\partial \Omega}\epsilon_\Omega\right)^2}$. The calibration of the five-hole probe, including the recovery factor at the temperature sensor, leads to further uncertainties according to the residuals of the calibration polynomials which are added at this point to the error of the processed results. The error propagation is continued up to the integration of the wake data. As the utilised trapezoidal integration is based on a sectional linear interpolation of the measurement points, the wake curve can be interpreted as sectionally differentiable. Consequently, a corresponding error can be determined for each position along the wake. For the integration of the flow quantities in the wake, linear error propagation has to be applied: $\epsilon_I = \sum_{i=1}^{N} \frac{\partial I}{\partial \Omega_i}\epsilon_{\Omega_i}$. It can be assumed that further errors of discretisation are low due to the high resolution of measurement points within the wake. The further data processing, however, underlies Gaussian error propagation. With this process, the resulting measurement uncertainty for the averaged loss coefficient is dependent on the operating point, the averaging technique and, finally, the definition of the loss coefficient. In Table 1 the cases with the respective highest and lowest absolute error values concerning the presented results at high temperatures are shown.

4.0 APPLICATION OF LOSS DEFINITIONS AND AVERAGING TECHNIQUES

The presented investigations are targeted to find the best way to evaluate the profile loss at a blade row under consideration of heat transfer into the flow. Additionally, some aerodynamic conclusions can be drawn. Finally, the transferability of the results to cases with superimposed endwall losses was investigated.

4.1 Comparison of loss coefficients

In Fig. 6 the discussed definitions of the loss coefficient for wake traverses at the cascade's mid-span at medium inflow Mach number and high Reynolds number at different heating levels are shown. All results are based on an identical data set. The heating power is normalised to the air mass flow per passage for a better comparability of different inflow Mach and Reynolds numbers.

At first sight, it is obvious that the energy and entropy loss coefficients show a distinct, almost linear progress with increased heating power per passage mass flow while the total pressure loss coefficient as well as the extended enthalpy loss coefficient only show a slight elevation with increased heating power. In approaches that consider the temperature elevation in the wake, it can be furthermore observed that the inclination of the extended enthalpy loss coefficient is higher than the one of the total pressure loss coefficient. This indicates that losses caused by thermal mixing are not adequately considered utilising the total pressure loss coefficient.

This progress of the loss coefficient with increasing heating power is reasonable, taking the Reynolds number dependency of the loss coefficient into account. A higher temperature of

https://doi.org/10.1017/aer.2020.57 Published online by Cambridge University Press

Table 1
Measurement uncertainty of averaged loss coefficients (absolute values)

	Medium Mach. High Reynolds		Low Mach. Low Reynolds	
	total pressure	extended enthalpy	total pressure	extended enthalpy
mass flow average	0.19%	0.23%	0.52%	0.54%
mixed-out average	0.19%	0.27%	0.52%	0.66%

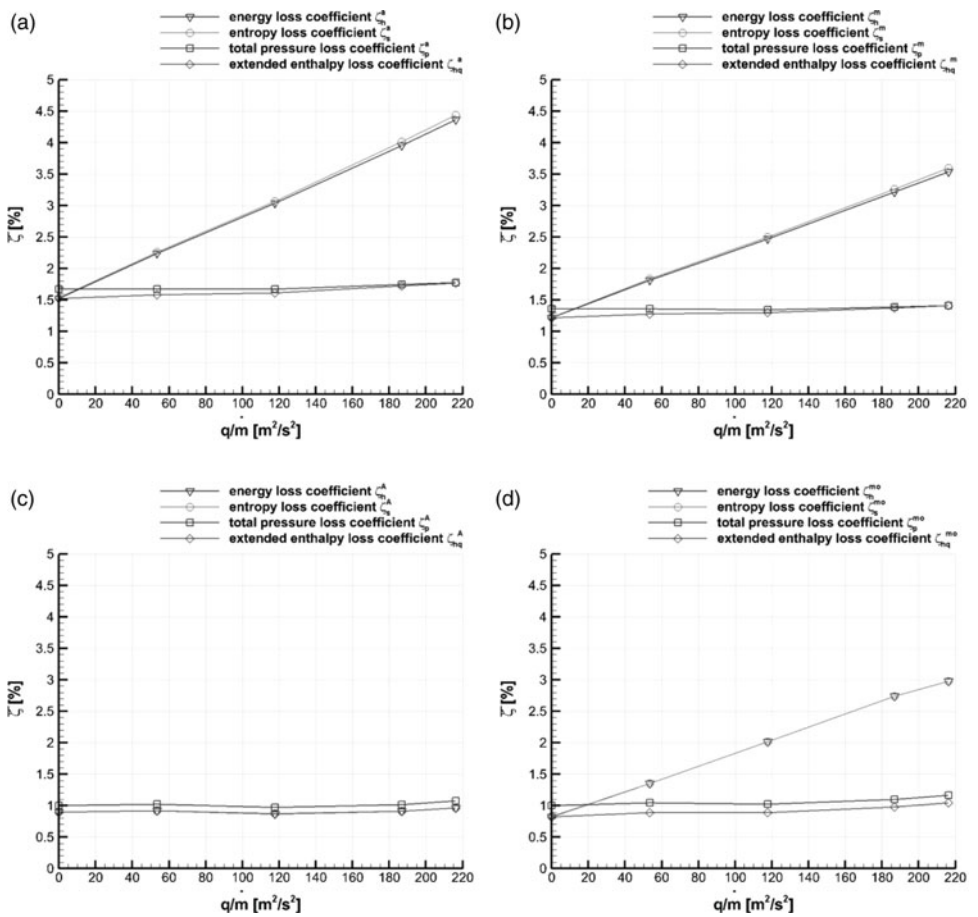

Figure 6. Comparison of different definitions of the loss coefficient, shown for different averaging techniques; operating point: medium Mach number, high Reynolds number. (6a) Area-weighted average. (6b) Mass flow-weighted average. (6c) Amecke average. (6d) Complete mixed-out average

the blade surface leads to a locally higher flow temperature inside the boundary layer while a higher air temperature means a higher viscosity according to Sutherland[21] and, thus, a lower local Reynolds number on the blade surface. Provided that the loss coefficient is decreasing with increasing Reynolds number per chord length due to the displacement of boundary layer

https://doi.org/10.1017/aer.2020.57 Published online by Cambridge University Press

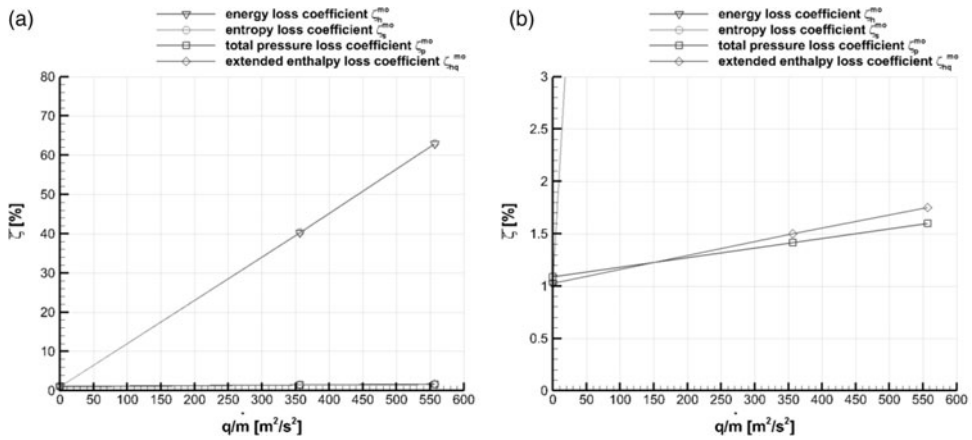

Figure 7. Comparison of different definitions of the loss coefficient; operating point: low Mach number, low Reynolds number. (7a) Complete mixed-out average: Full range; (7b) Complete mixed-out average: Zoomed-in.

transition as was shown by Mayle,[22] it is reasonable that a higher blade temperature with a lower local Reynolds number leads to a higher loss.

Comparing the different averaging techniques, the area- and mass flow-weighted average follow similar distributions while the mass flow-weighted average is always lower than the area-weighted average. This is conformable to the theory, as the loss at boundary layers is overrated by the area-weighted average. Cumpsty and Horlock[7] have already shown that for the evaluation of enthalpy information, the usage of the area-weighted average is only justified, if the deviation to the more reasonable mass flow-weighted average is low which is not the case for the presented experiments here.

Furthermore, it is noteworthy that with the Amecke average as well as with the complete mixed-out average, the energy and entropy loss coefficient fit nearly exactly together, whereas for the area-weighted average and the mass flow-weighted average both distributions are only similar. Thus, the mixed-out averaging techniques lead to physically more coherent results, as the energy and entropy loss coefficient always have to be approximately equal according to Denton[2].With the Amecke average, also the extended enthalpy loss coefficient is approximately equal to the energy and entropy loss coefficient. This is due to the fact that the temperature gradient is ignored by the approach of Amecke and the extension term Δh_q in Equation 14a is zero. While for both mixed-out averaging techniques, the extended enthalpy loss coefficient is lower than the total pressure loss coefficient, the offset between both is almost constant with the Amecke average. As this difference is getting lower with increased heating power, using the complete mixed-out average, the fact that the Amecke average can only be a reasonable method for non-adiabatic wake-traverses, if the impact of the temperature gradient is low, is underscored. Hence, the complete mixed-out average is in focus of the following evaluations.

The tendencies pointed out in Fig. 6 for different averaging techniques can analogously be shown for other operating points. Comparing the definitions of the loss coefficient in the case of a low inflow Mach number and low Reynolds number, as depicted in Fig. 7, the difficulty of the usage of the so far established energy and entropy loss coefficient at non-adiabatic test articles is obvious. The loss of energy is interpreted as extensively high while the local values of the loss in the wake raise up to 500%. It is needless to say that a loss higher than

https://doi.org/10.1017/aer.2020.57 Published online by Cambridge University Press

Table 2
Overview of suitable combinations of loss coefficient definitions and averaging techniques for a non-adiabatic flow

		area avg. $\bar{\zeta}^{a}$	mass flow avg. $\bar{\zeta}^{m}$	Amecke avg. $\bar{\zeta}^{A}$	complete mixed-out avg. $\bar{\zeta}^{mo}$
energy	ζ_h	×	×	!	×
entropy	ζ_s	×	×	!	×
total pressure	ζ_p	!	✓	!	✓
extended enthalpy	ζ_{hq}	!	✓	!	✓

✓ : suitable
! : suitable with restrictions
× : not suitable

100% is not reasonable. This confirms that the extension of the definition of the enthalpy loss coefficient is necessary for its correct interpretation. The distinct increase of the energy loss coefficient is only due to the misinterpreted energy addition as loss. However, by applying the extended enthalpy loss coefficient, a sound assessment of the aerodynamic loss behaviour is enabled, leading to a similar order of magnitude as the total pressure loss coefficient.

In contrast to the measurements at higher inflow Mach number, the extended enthalpy loss coefficient is higher than the total pressure loss coefficient at high blade temperatures. It is the other way around for the cold blade, although, as to the theory, all loss coefficients have to deliver equal results for adiabatic and incompressible cases. The results indicate that a further rise of the temperature gradient between blade and flow would cause a further increase of the profile loss and might also lead to an intersection of the curves of both loss definitions for the medium inflow Mach number. Additionally, it can be assumed that the difference between both loss definitions correlates with the influence of compressibility, beside the consideration of heat transfer. If the extended enthalpy loss coefficient is higher than the total pressure loss coefficient, the impact of the heat addition on the loss is higher than effects of compressibility. Anyway, it can be useful to consider both values for the interpretation of aerodynamic data.

4.2 Rating of loss coefficients for non-adiabatic cases

In all, it turned out that different definitions of the loss coefficient and different averaging techniques cannot be evaluated fully independently from each other. To give an overview, of the former presented results to the suitability of different approaches, the respective combinations are rated in Table 2. The main assessment criterion for the presented methods is their thermodynamic validity. Additionally, their robustness, which is highly correlated to their measurement uncertainty, is an important measure of the specific suitability.

It was shown above that the energy loss coefficient is not a suitable measure, if a temperature increase is present, as this is erroneously counted as loss. For low-temperature variations, the Amecke average can be a suitable measure, accepting that the temperature increase is fully neglected. The same arguments apply for the entropy loss coefficient. As to the total pressure loss coefficient and the extended enthalpy loss coefficient, the area-weighted average is only

https://doi.org/10.1017/aer.2020.57 Published online by Cambridge University Press

Table 3
Robustness of loss coefficient definitions and averaging techniques

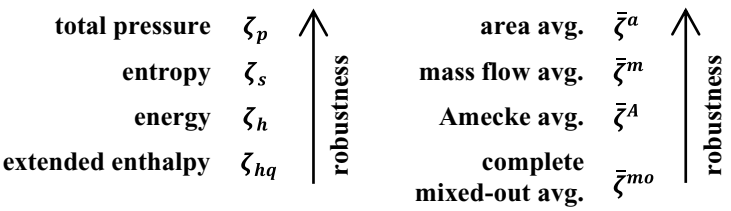

suitable, accepting too, that the mass deficit in the wake is not accounted for. This, however, is considered by the mass flow-weighted average. As well, the complete mixed-out average leads to reasonable results, whereas the Amecke average is only suitable, if the temperature increase is consciously not to be considered.

Beside theoretical considerations on the reasonability of the discussed methods, their robustness might be an additional argument which is summarised in Table 3. This applies particularly for experimental data, as a loss definition is not necessarily suitable, if a low change of the input data due to measurement uncertainties effects a high change in the resulting loss coefficient. It was found that all definitions of the loss coefficient which imply a temperature measurement are more sensitive to measurement uncertainties than methods based on pressure data only. For the presented operating points, the pressure measurements are more accurate in relation to the measured value, than measurements of the total temperature. Hence, the higher the temperature information is weighted for the respective loss coefficient, the less robust is its reliable calculation. As to the mixed-out averaging techniques, the solution of the conservation equations leads to comparably complex mathematic results, effecting that the measurement uncertainties sum up to higher orders. This means, that although the complete mixed-out averaged extended enthalpy loss coefficient might be physically the most reasonable measure, a more robust measure, such as the mass flow averaged total pressure loss coefficient, might give more reliable results, if measurement uncertainties are high. In this concern, the acceptable uncertainty is highly dependent on the operation point and on the intended purpose of the evaluation. With measurement uncertainties within the typically occurring range, the presented ranking is consistently applicable and supports as a guideline in choosing the respective most suitable measure.

4.3 Transfer to field traverses

The previously presented results were gained from wake traverses at the cascade's mid-span while focussing on the investigation of the profile loss. The conduction of field traverses over the entire blade span often deals with superimposed endwall losses or, in special cases, as well with leakage losses. Details on these loss mechanisms are also shown by Denton[2]. The secondary flow near the endwalls typically cause high losses. Here, the gradients in total pressure are mostly higher than for wake traverses at mid-span, because these are only influenced by the profile loss. Therefore, the question about the reasonability of the mass flow-weighted average for total pressure data arises. Moreover, it was already shown that the area-weighted average of the loss parameter is not reasonable in this case as well. The implementation of the complete mixed-out average compared to the Amecke average, however, enables the evaluation of field traverses by a further, promising method. Similar as for single wake traverses, it could be shown that energy and entropy loss coefficient fit best by this approach.

https://doi.org/10.1017/aer.2020.57 Published online by Cambridge University Press

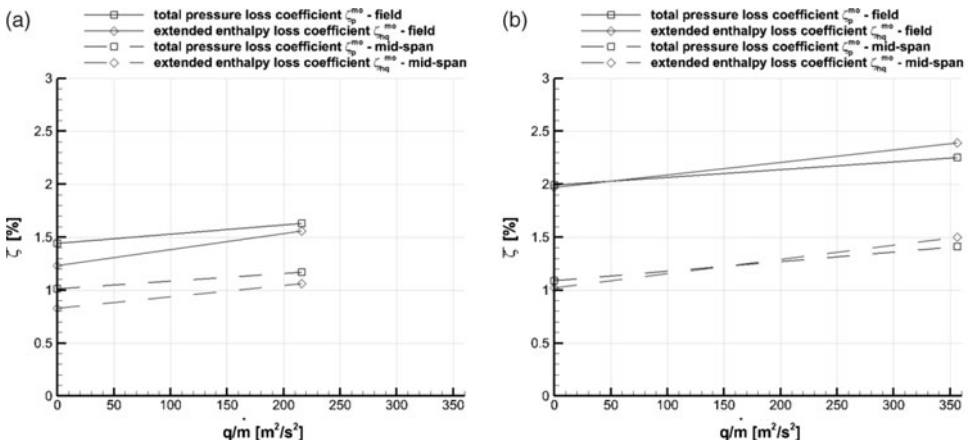

Figure 8. Completed mixed-out averaged loss coefficients for field traverses and single wake traverses at mid span, each for a cold and a hot blade at similar blade temperatures. (8a) Medium Mach number, high Reynolds number. (8b) Low Mach number, low Reynolds number.

In Fig. 8 the extended enthalpy loss coefficient is compared to the total pressure loss coefficient for field traverses at two operating points. The field includes initial parts of secondary flow at both blade ends but does not represent the endwall losses entirely. From these measurements, it is obvious that both presented loss coefficients for field traverses are rising with increased heating power, similar as for a single wake measurement. Furthermore, the gradient of the extended enthalpy loss coefficient seems to be higher for the field traverse than for the single wake traverse. In contrast to that, this is not indicated by the total pressure loss coefficient.

5.0 CONCLUSIONS

The combination of the loss characterisation of a linear cascade by wake traverses with heat transfer on the blade is a challenging task as typical measurement and evaluation techniques are based on the assumption of an adiabatic flow. Therefore, novel and powerful methods were developed to enable the measurement and evaluation of non-adiabatic wake traverses. In focus of this approach was to find a method that is not only thermodynamically valid but also independent from an adiabatic reference case and can be determined from airfoil wake data. From an experimental test case, the following conclusions can be drawn:

1. The energy and entropy loss coefficient according to Denton[2] is not suitable for non-adiabatic cases, as an increased temperature in the wake is counted as pure loss.
2. Instead the new introduced extended enthalpy loss coefficient according to Equation 15 can be used.
3. The total pressure loss coefficient can also be suitable, taking into account that energetic effects are not represented entirely.
4. The definitions of the loss coefficient and corresponding averaging techniques cannot be evaluated fully independently from each other.
5. As an established averaging technique, the mass flow-weighted average is pointed out as a suitable measure for non-adiabatic cases.

https://doi.org/10.1017/aer.2020.57 Published online by Cambridge University Press

6. Additionally, the complete mixed-out average according to Equations 10, 11, 12, 23 and 24 turned out as physically even more reasonable but less robust than the mass flow-weighted average.
7. The mixed-out average by Amecke[8] does not account for a temperature gradient in the wake but leads to similar results as the complete mixed-out average for small heat addition values in relation to the operating point.
8. Not only is the physical reasonability of a loss definition or an averaging technique to be considered for a suitable choice but also the robustness of their calculation which correlates with the accuracy of measurement.
9. Concerning the presented test results, the loss definitions and averaging approaches are the less robust, the more the measured temperature is weighted for the resulting loss coefficient. Hence, high-precision temperature measurements are a prerequisite.
10. All conclusions are valid for single wake traverses as well as for area traverses.
11. These findings are based on a particular case of a compressor cascade (with and without blade heating). It is expected that they can be transferred to other cases as well.

With the presented considerations on the extended enthalpy loss coefficient as well as the complete mixed-out average, the energetically based evaluation of single wake and field traverses to characterise the loss of a turbomachinery component is enabled. Finally, an additional powerful procedure was found which gives detailed information on the influence of heat transfer to the wake and, thus, the aerodynamic loss which can be utilised to optimise engine efficiencies in the near future.

ACKNOWLEDGEMENTS

The investigations were conducted in cooperation with GE Aviation. The authors would like to thank GE for the permission to publish this data. This project has received funding from the Clean Sky 2 Joint Undertaking under the European Union's Horizon 2020 research and innovation program under grant agreement No CSJU-CS2-GAM-ENG-2014-15.

REFERENCES

1. GOMES, R. and NIEHUIS, R. Aerothermodynamics of a High-Pressure Turbine Blade With Very High Loading and Vortex Generators, *ASME Journal of Turbomachinery*, **134**, (1), 011020, 2012. https://doi.org/10.1115/1.4003052
2. DENTON, J.D. Loss mechanisms in turbomachines, *ASME Journal of Turbomachinery*, **115**, (4), pp 621–656, 1993. https://doi.org/10.1115/1.2929299
3. STOTZ, S., GUENDOGDU, Y. and NIEHUIS, R. Experimental investigation of pressure side flow separation on the T106C airfoil at high suction side incidence flow, *ASME Journal of Turbomachinery*, **139**, (5), 051007, 2017. https://doi.org/10.1115/1.4035210
4. SCHOBEIRI, M.T., GILARRANZ, J.L. and JOHANSEN, E.S. Aerodynamic and performance studies of a three-stage high pressure research turbine with 3-D - blades, design point and off-design experimental investigations, *Proceedings of ASME Turbo Expo: Power for Land, Sea, and Air*, 2000-GT-0484 Munich, Germany, May 8–11, 2000. https://doi.org/10.1115/2000-GT-0484
5. LIM, C.H., PULLAN, G. and NORTHALL J., Estimating the loss associated with film cooling for a turbine stage, *ASME Journal of Turbomachinery*, **134**, (2), 021011, 2012. https://doi.org/10.1115/1.4003255
6. GUNN, E.J. and HALL, C.A. Loss and deviation in windmilling fans, *ASME Journal of Turbomachinery*, **138**, (10), 101002, 2016. https://doi.org/10.1115/1.4033163

7. CUMPSTY, N.A. and HORLOCK, J.H. Averaging non-uniform flow for a purpose, *ASME Journal of Turbomachinery*, **128**, (1), pp 120–129, 2006. https://doi.org/10.1115/1.2098807
8. AMECKE, J. Auswertung von Nachlaufmessungen an ebenen Schaufelgittern, Technical Report 67A49, AVA Göttingen, Germany, 1967.
9. PRASAD, A. Calculation of the mixed-out state in turbomachine flows, *ASME Journal of Turbomachinery*, **127**, (3), pp 564–572, 2005. https://doi.org/10.1115/1.1928289
10. LEIPOLD, R., BOESE, M. and FOTTNER, L. The influence of technical surface roughness caused by precision forging on the flow around a highly loaded compressor cascade, *ASME Journal of Turbomachinery*, **122**, (3), pp 416–424, 2000. https://doi.org/10.1115/1.1302286
11. HILGENFELD, L. and PFITZNER, M. Unsteady boundary layer development due to wake passing effects on a highly loaded linear compressor cascade, *ASME Journal of Turbomachinery*, **126**, (4), pp 493–500, 2004. https://doi.org/10.1115/1.1791290
12. LEGGETT, J., PRIEBE, S., SHABBIR, A., MICHELASSI, V., SANDBERG, R. and RICHARDSON, E. Loss prediction in an axial compressor cascade at off-design incidences with free stream disturbances using large eddy simulation, *ASME Journal of Turbomachinery*, **140**, (7), 071005, 2018. https://doi.org/10.1115/1.4039807
13. HOWELL, R.J. and ROMAN, K.M. Loss reduction on ultra high lift low-pressure turbine blades using selective roughness and wake unsteadiness, *The Aeronautical Journal*, **111**, (1118), pp 257–266, 2007. https://doi.org/10.1017/S0001924000004504
14. PIANKO, M. and WAZELT, F. Propulsion and energetics panel working group 14 on suitable averaging techniques in non-uniform internal flows, Advisory Group for Aerospace Research and Development, No. AGARD-AR-182, 1983.
15. STRUTT, J.W. (Lord Rayleigh) Aerial plane waves of finite amplitudes, *Proceedings of the Royal Society of London A*, **84**, (570), pp 247–284, 1910. https://doi.org/10.1098/rspa.1910.0075
16. KOST, F. *Längswirbelentstehung in einem Turbinenlaufrad mit konischen Seitenwänden*, PhD thesis, DLR Cologne, 1993.
17. SCHLICHTING, H. The variable density high speed cascade wind tunnel of the Deutsche Forschungsanstalt für Luftfahrt Braunschweig, Advisory Group for Aerospace Research and Development, AGARD-Report Nr. 91, 1956.
18. STURM, W. and FOTTNER, L. The high-speed cascade wind-tunnel of the German Armed Forces University Munich, *8th Symposium on Measuring Techniques for Transonic and Supersonic Flows in Cascades and Turbomachines*, Genoa, Italy, 1985.
19. ABERLE, S., BITTER, M., HOEFLER, F., CARRETERO BENIGNOS, J. and NIEHUIS, R. Implementation of an in-situ infrared calibration method for precise heat transfer measurements on a linear cascade, *ASME Journal of Turbomachinery*, **141**, (2), 012004, 2019. https://doi.org/10.1115/1.4041132
20. BARLOW, R.J. *Statistics: A Guide to the Use of Statistical Methods in the Physical Sciences, Vol.* 29, John Wiley & Sons, 1993. https://doi.org/10.1002/piuz.19910220112
21. SUTHERLAND, W. The viscosity of gases and molecular force, *Philosophical Magazine Series 5*, **36**, (223), pp 507–531, 1893. https://doi.org/10.1080/14786449308620508
22. MAYLE, R.E. The role of laminar-turbulent transition in gas turbine engines, *Proceedings of ASME 1991 International Gas Turbine and Aeroengine Congress and Exposition*, 91-GT-261, Orlando, FL, June 3–6, 1991. https://doi.org/10.1115/91-GT-261